



**HAL**  
open science

## Study of electrical properties and estimation of average mobility and diffusion coefficients in several insulating liquids by dielectric spectroscopy

Xavier Sidambarompoulé, Petru Notingher, Thierry Paillat, Jean-Charles Laurentie, Paul Leblanc

### ► To cite this version:

Xavier Sidambarompoulé, Petru Notingher, Thierry Paillat, Jean-Charles Laurentie, Paul Leblanc. Study of electrical properties and estimation of average mobility and diffusion coefficients in several insulating liquids by dielectric spectroscopy. *International Journal of Plasma Environmental Science and Technology*, 2020, 14 (3), pp.e03006. 10.34343/ijpest.2020.14.e03006 . hal-03224002

**HAL Id: hal-03224002**

**<https://hal.science/hal-03224002>**

Submitted on 31 Mar 2022

**HAL** is a multi-disciplinary open access archive for the deposit and dissemination of scientific research documents, whether they are published or not. The documents may come from teaching and research institutions in France or abroad, or from public or private research centers.

L'archive ouverte pluridisciplinaire **HAL**, est destinée au dépôt et à la diffusion de documents scientifiques de niveau recherche, publiés ou non, émanant des établissements d'enseignement et de recherche français ou étrangers, des laboratoires publics ou privés.

# Study of electrical properties and estimation of average mobility and diffusion coefficients in several insulating liquids by dielectric spectroscopy

Xavier Sidambarompoulé<sup>1,\*</sup>, Petru Notingher<sup>1</sup>, Thierry Paillat<sup>2</sup>,  
Jean-Charles Laurentie<sup>1</sup>, Paul Leblanc<sup>2</sup>

<sup>1</sup> Université de Montpellier, CNRS, Montpellier, France

<sup>2</sup> Université de Poitiers, CNRS, Poitiers, France

\* Corresponding author: [xavier.sidambarompoule@umontpellier.fr](mailto:xavier.sidambarompoule@umontpellier.fr) (Xavier Sidambarompoulé)

Received: 2 December 2020

Revised: 13 December 2020

Accepted: 13 December 2020

Published online: 16 December 2020

## Abstract

Electrical properties of cyclohexane, a pure mineral oil, a mineral oil with additive and a silicon oil are studied in the frequency range of  $10^{-2} - 10^5$  Hz. The paper reviews theoretical and practical basics for wide range dielectric spectroscopy measurements and puts into focus a method for estimating ionic mobility and diffusion coefficients in insulating liquids via data issued from low frequency spectra. Results obtained at different temperatures are presented and discussed.

**Keywords:** Dielectric liquid, spectroscopy, permittivity, electrode polarization, conductivity, mobility, diffusion coefficient.

## 1. Introduction

Electrical conductivity, charge mobility and diffusion coefficients are useful elements for studying and modeling electrical behavior of insulating liquids and for embedding these materials in various applications. These parameters vary largely with temperature and are strongly dependent on water and impurity contents [1 and references herein]. Charge carriers in insulating liquids are mainly due to the inherent presence of impurities in pure dielectric liquids leading to ion dissociation, rather than to the dissociation of the molecules of the liquid. Carrier mobility and diffusion coefficients, needed for charge and conduction modeling, are usually difficult to estimate, especially in highly insulating liquids. They are mainly approached through measurements of transient and/or stationary currents with respect to time under square voltage waves or increasing dc voltage [2–6]. Measurements of the currents due to the displacement of the concerned carriers under the effect of external radiation or electrical impulses are also used [4, 7].

On the other hand, dielectric spectroscopy [7, 8] is a well-known characterization technique, commonly used for measuring permittivity and loss factor and for studying relaxation phenomena in liquids [1, 7–11]. However, despite extensive theoretical consideration and modelling (e.g. [1 and references herein]), the performance of dielectric spectroscopy instruments has limited for long time obtaining and using dielectric spectroscopy data from the low frequency domain. With the aid of now widely available instrumentation, allowing exploring frequency ranges down to  $10^{-3}$  Hz and below, thorough analysis of thus obtained and sometimes-neglected data may allow direct determination of electrical conductivity and other useful related parameters of insulating liquids. This subject is addressed in this work.

Electrical properties of some generic insulating liquids are studied in the present paper via dielectric spectroscopy at different temperatures. Theoretical and practical aspects related to dielectric spectroscopy and its application to dielectric liquids are reviewed and a method usable for determining ionic mobility and diffusion coefficients in such substances from data derived from low frequency spectra is described. The technique is applied to the study of low-conductivity liquids (cyclohexane, mineral and silicon oils) and to a mineral oil for which conductivity is modified at different degrees with an additive.

## 2. Experimental aspects and data analysis

### 2.1 Dielectric liquids

The experiments described herein after have been carried out on three highly insulating liquids with different properties, particularly in terms of density and dynamic viscosity. The first one is cyclohexane, an alicyclic hydrocarbon from the family of (mono) cycloalkanes. Because it is a common, pure and widely available substance with well-known mechanical and thermal properties, cyclohexane was used as a test reference model. The values of its volume density  $\rho_m$ , dynamic viscosity  $\mu_{dyn}$ , thermal conductivity  $\lambda$ , heat capacity  $C_p$  and thermal diffusivity  $D_{th}$  at room temperature and atmospheric pressure are recalled in Table 1. Cyclohexane possesses a low dynamic viscosity. The variations of density and dynamic viscosity with temperature  $T$  in cyclohexane obey to the following laws [12]:

$$\rho_m(T) = 84.1595 \times \frac{0.8908}{0.27396^{1+\left(1-\frac{T}{553.58}\right)^{0.2851}}} \text{ kg/m}^3 \quad (1)$$

$$\mu_{dyn}(T) = \exp\left(-6.2946 + \frac{2340.16}{(80.1952+T)}\right) \times 0.001 \text{ Pa}\cdot\text{s} \quad (2)$$

Table 1. Thermal and mechanical properties of cyclohexane at 20°C under normal pressure [12, 13].

$\rho_m$ (kg m <sup>-3</sup> )	$\mu_{dyn}$ (Pa·s)	$\lambda$ (Wm <sup>-1</sup> K <sup>-1</sup> )	$C_p$ (J kg <sup>-1</sup> K <sup>-1</sup> )	$D_{th}$ (m <sup>2</sup> s <sup>-1</sup> )
778	$9.76 \times 10^{-4}$	0.2	1850	$1.38 \times 10^{-7}$

The second substance is a Shell Diala S2 mineral oil, employed on a large scale in electrical engineering, especially as an electrically insulating and cooling agent for power transformers. This is a typical dielectric liquid, made of an assembly of highly refined hydrocarbons, and which does not oxidize when put into contact with copper (hence its interest as transformer oil). Its dynamic viscosity is 20 times higher than that of cyclohexane. Its thermal and mechanical properties at 20°C under normal pressure are given in Table 2. The variation of its density can be considered as proportional to temperature, with a variation coefficient  $\beta = (1/\rho_m) \times (\partial\rho_m/\partial T) = 7 \times 10^{-4} \text{ K}^{-1}$  [14].

Table 2. Thermal and mechanical properties of the studied mineral oil at 20°C under normal pressure [14].

$\rho_m$ (kg m <sup>-3</sup> )	$\mu_{dyn}$ (Pa·s)	$\lambda$ (Wm <sup>-1</sup> K <sup>-1</sup> )	$C_p$ (Jkg <sup>-1</sup> K <sup>-1</sup> )	$D_{th}$ (m <sup>2</sup> s <sup>-1</sup> )	$\beta$ (K <sup>-1</sup> )
850	$17 \times 10^{-3}$	0.15	1900	$9.28 \times 10^{-8}$	$7 \times 10^{-4}$

In the present study, this oil has been analyzed both in its original state (without any additive) and after adding small quantities of an additive in order to observe the resulting modifications in conductivity, mobility and charge diffusion, both for studying purposes and for assessing the procedure proposed for their determination. The used additive was OLOA 218, a calcium phenate for which the reactions taking place at its dissolution in oils lead to the appearance of ionic carriers, whose presence, even in a very limited amount, is able to increase oil conductivity significantly. Three mineral oil/additive solutions were prepared, with OLOA 218 concentrations of 5 ppm, 10 ppm and 20 ppm, respectively. They were obtained from a “mother” solution containing 0.1 % of additive in volume, which was elaborated in a first step and diluted thereafter in pure oil to reach the desired concentrations.

A silicon oil (Rhodorsil 47V50 [15]) was also studied. This is a poly-dimethyl siloxane, used in high voltage applications for its dielectric properties, its thermal stability and its lubricating properties [16]. As for the other liquids, its thermal and mechanical characteristics at room temperature and normal pressure are given below. Its viscosity is three times higher than the one of mineral oil and nearly two orders of magnitude above that of cyclohexane.

Table 3. Thermal and mechanical properties of the studied silicon oil at 20°C under normal pressure [14].

$\rho_m$ (kg m <sup>-3</sup> )	$\mu_{dyn}$ (Pa·s)	$\lambda$ (Wm <sup>-1</sup> K <sup>-1</sup> )	$C_p$ (J kg <sup>-1</sup> K <sup>-1</sup> )	$D_{th}$ (m <sup>2</sup> s <sup>-1</sup> )	$\beta$ (K <sup>-1</sup> )
959	$47.9 \times 10^{-3}$	0.16	1460	$1.14 \times 10^{-7}$	$1.05 \times 10^{-3}$

## 2.2 Measurement cell, apparatus and procedure

Each sample was composed of 200 ml of liquid, which was carefully poured into an *IRLAB CL-1* cell (Fig. 1), designed and manufactured in accordance with the IEC 60247 recommendations [17, 18]. Two coaxial electrodes are immersed in the liquid and connected to the measuring device for applying an ac voltage and measuring the response current. The dimensions of the cell are the following:

- Inner diameter of the outer electrode: 50.1 mm
- Outer diameter of the inner electrode: 42.7 mm
- Distance between the two cylindrical electrodes: 3.7 mm
- Height of the electrodes: 62.1 mm

For measurements at temperatures other than room temperature, the cell was set into a thermostatically controlled tank filled with a liquid at the desired temperature. For this purpose, the cell has been modified to make it liquid-tight. The sample temperature has been continuously controlled via a sensor inserted into the cell (Fig. 1).

The measurement data was acquired via a Solartron Analytical Modulab MTS spectrum analyzer equipped with a “low current” module, which can be used in a frequency range from 10  $\mu$ Hz to 1 MHz to measure current values lower than the pA with resolutions down to 0.15 fA. The complex capacitance of the samples was measured in a frequency range from 10 mHz to 100 kHz, under an applied sinusoidal voltage of Root Mean Square value of 10 V. This low voltage has been chosen in order to avoid charge injection at electrodes. The measurement were made in a temperature range of 8°C to 50°C for mineral and silicon oil and of 45°C to 50°C for cyclohexane.

Empty cell measurements were carried out to validate the measurement system. The cell documentation gives an empty cell capacitance of 22.3 pF at 0.5 Hz [18]; this value has been checked at three temperatures: 13°C, 20°C and 30°C (Fig. 2). The differences between the values measured at these temperatures are of the order of 0.1% at the most. For such a capacitance, the precision of the spectrometer is 0.25%. Thus, the observed difference is in the range of the measurement device precision, the dispersion being low enough not to need corrections.

A strict protocol was observed to avoid sample contamination by foreign substances, which may highly affect measurement results. Thus, before pouring in any new liquid sample, the cell was cleaned with heptane (a hydrocarbon used as a solvent, which has the particularity of dissolving oily liquids, but which is also volatile enough to evaporate in open air). A calibration measurement of the capacitance of the empty cell was then systematically carried out. In order to eliminate all traces of impurities that may pollute the sample liquid, the cell was then filled and emptied twice with the “new” liquid to be characterized, before being definitively filled for the measurements.

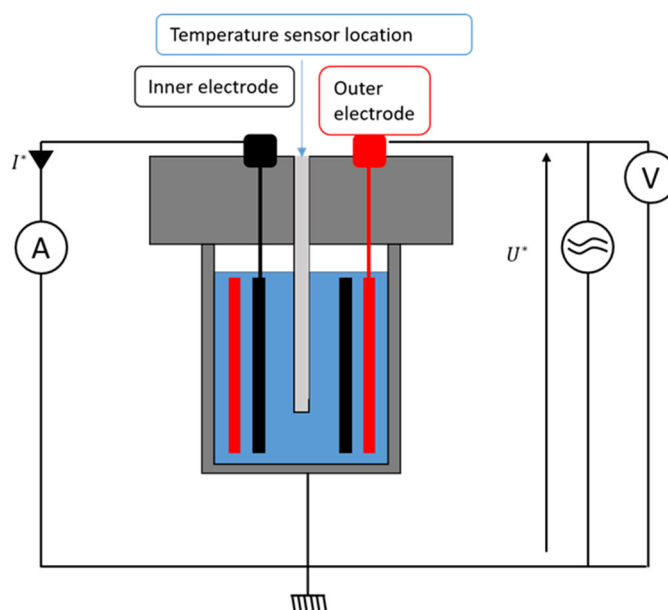


Fig. 1. Diagram of the measurement cell and circuit.

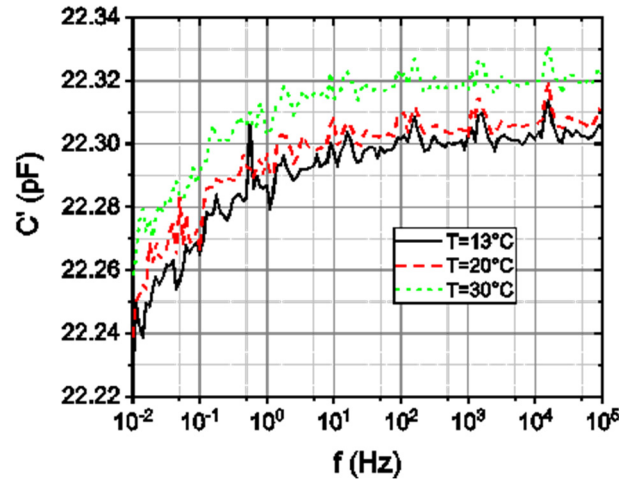


Fig. 2. Capacitance spectrum of the empty measurement cell.

### 2.3 Analysis of measured data and determination of electrical conductivity, ionic mobility and diffusion coefficient

For a given frequency  $f$  (or angular frequency  $\omega = 2\pi f$ ), a sinusoidal voltage  $u(t) = U_{RMS}\sqrt{2}\sin(\omega t)$  is applied to the sample by the spectroscope, and the current  $i(t) = I_{RMS}\sqrt{2}\sin(\omega t - \phi)$  issued from the sample in permanent regime is measured by the instrument.  $U_{RMS}$  designates here the Root Mean Square value of  $u(t)$ ,  $I_{RMS}$  the root mean square value of  $i(t)$  and  $\phi$  the phase shift of  $u(t)$  with respect to  $i(t)$ . The complex impedance of the sample reads:

$$Z^* = \frac{U^*}{I^*} \tag{3}$$

where  $U^*$  and  $I^*$  are the complex values associated to  $u(t)$  and  $i(t)$ , respectively. The complex capacitance  $C^*$  associated to the sample is defined such as:

$$Z^*(\omega) = \frac{1}{j\omega C^*(\omega)} \tag{4}$$

so:

$$C^*(\omega) = \frac{1}{j\omega Z^*(\omega)} \tag{5}$$

$C^*$  can be written as:

$$C^*(\omega) = C'(\omega) - jC''(\omega) \tag{6}$$

where  $C'$  is the real part and  $C''$  the imaginary part of  $C^*$ . On the other hand:

$$C^*(\omega) = \epsilon_r^*(\omega)C_0 = [\epsilon_r'(\omega) - j\epsilon_r''(\omega)]C_0 \tag{7}$$

where  $\epsilon_r^*$  is the complex relative permittivity of the liquid (with its real and imaginary parts  $\epsilon_r'$  and  $\epsilon_r''$ ) and  $C_0$  is the capacitance of the empty cell. The relationship between the complex permittivity of the liquid  $\epsilon_r^*$ ,  $Z^*$  and  $C_0$  is then:

$$\epsilon_r^*(\omega) = \frac{C^*(\omega)}{C_0} = \frac{1}{j\omega Z^*(\omega)C_0} \tag{8}$$

The real and imaginary parts of the relative permittivity read:

$$\varepsilon_r'(\omega) = \frac{C'(\omega)}{C_0}, \quad \varepsilon_r''(\omega) = \frac{C''(\omega)}{C_0} \quad (9)$$

and the loss factor is:

$$\tan\delta(\omega) = \frac{\varepsilon_r''(\omega)}{\varepsilon_r'(\omega)} = \frac{C''(\omega)}{C'(\omega)} \quad (10)$$

Thus, after measuring the complex impedance of the empty cell and of the liquid sample, the relative permittivity and the loss factor of the liquid in the considered frequency range can be determined by using the above relationships [7, 19].

The more or less important displacements of the free charge carriers (i.e., the liquid ions) also allow determining the conductivity of the liquid. Indeed, the complex conductivity of the material  $\sigma^*$  is defined as the ratio between the complex relative permittivity  $\varepsilon_r^*$  and the impedance of the empty cell  $Z_0$  [7, 19]

$$\sigma^* = \frac{\varepsilon_r^*}{Z_0} = \varepsilon_r^* j\omega\varepsilon_0 = \sigma' + j\sigma'' \quad (11)$$

where  $\varepsilon_0$  is the permittivity of the air,  $\sigma'$  is the real part of the conductivity and  $\sigma''$  its imaginary part. Consequently:

$$\sigma'(\omega) = \omega\varepsilon_0\varepsilon_r''(\omega), \quad \sigma''(\omega) = \omega\varepsilon_0\varepsilon_r'(\omega) \quad (12)$$

When  $\omega \rightarrow 0$ ,  $\sigma'$  approaches the static conductivity (also called “direct current conductivity”)  $\sigma_{DC}$ , which is the « genuine » conductivity of the material. Therefore,  $\sigma_{DC}$  can be determined by analyzing the low frequency region of the real conductivity spectrum and identifying the plateau where  $\sigma'$  is constant.

As far as permittivity is concerned, when the frequency of the electric field applied to the material becomes very low, all the dipolar sub-molecular, molecular and supra-molecular entities are able to follow the variations of the field. Consequently, the permittivity of the material does not change anymore when the frequency decreases. This leads to a plateau in the spectrum of  $\varepsilon_r'(\omega)$  (Fig. 3). If the movements of these bonded charges need much less energy than those of the free carriers, the effects in term of losses are mostly due to conduction. As from the previous equation it comes out that  $\varepsilon_r''(\omega) = 1/(\omega\varepsilon_0\sigma'(\omega))$ , if  $\sigma'(\omega) = \sigma_{DC} = \text{constant}$ , the variation of  $\log(\varepsilon_r'')$  is inversely proportional to  $\omega$ . Consequently, the graphical representation of  $\log(\varepsilon_r'')$  versus  $\log(\omega)$  is a line of slope equal to  $-1$  (as shown in the middle part of Fig. 3). Therefore, the static conductivity  $\sigma_{DC}$  can be determined by analyzing the low frequency spectra of the liquid and by identifying the presence of the region where the real permittivity  $\varepsilon_r'$  is constant and the logarithm of the imaginary permittivity  $\varepsilon_r''$  varies linearly with a slope of  $-1$ .

However, such a region may not be visible in the spectra (depending on the frequency limits of the spectroscope and on the value of the material conductivity), or may be accompanied by a region where the real permittivity starts to vary again and the slope of the imaginary permittivity decreases in absolute value (Fig. 3, left part). Indeed, if the transit time of the charges between the electrodes is lower than the voltage half-cycle, the free carriers set into movement by the electric field may have enough time to reach the electrodes of opposite sign and to accumulate at the liquid/electrode interfaces. Consequently, a space charge polarization sets up at electrodes (i.e., electrode polarization), which is illustrated in the spectra by an increase of  $\varepsilon_r'$  and by a slope of  $\log(\varepsilon_r'') = f(\log(\omega))$  which may become greater than  $-1$  when the frequency diminishes (Fig. 3). As far as the relaxation processes are concerned, they usually have smaller time constants and appear therefore higher in the spectra. On the other hand, the conductivity of the studied material can also be determined by tracing the spectra of  $\sigma'$  and  $\sigma''$  and by identifying the low frequency range where  $\sigma'$  is constant, as indicated before (Fig. 4).

The value of the frequency corresponding to the onset of electrode polarization can be used to estimate the average transit time of ions between electrodes, from which their average mobility and diffusion coefficient can be calculated. Under a uniform sinusoidal field, Tobazéon [3] has shown that this transit time  $t_t$  is:

$$t_t = \sqrt{\frac{\sqrt{2}d^2}{\mu_{ion}\omega U_{RMS}}} \quad (13)$$

with  $d$  the inter-electrode distance and  $\mu_{ion}$  the average ionic mobility.

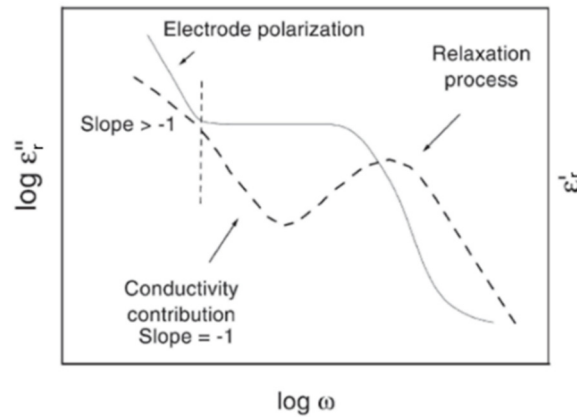


Fig. 3. Spectral signature of the real ( $\epsilon_r'$  - solid line) and imaginary ( $\epsilon_r''$  -- dotted line) parts of relative permittivity with respect to angular frequency  $\omega$ , corresponding to a unique relaxation mechanism (Debye) combined to conduction and electrode polarization mechanisms [7].

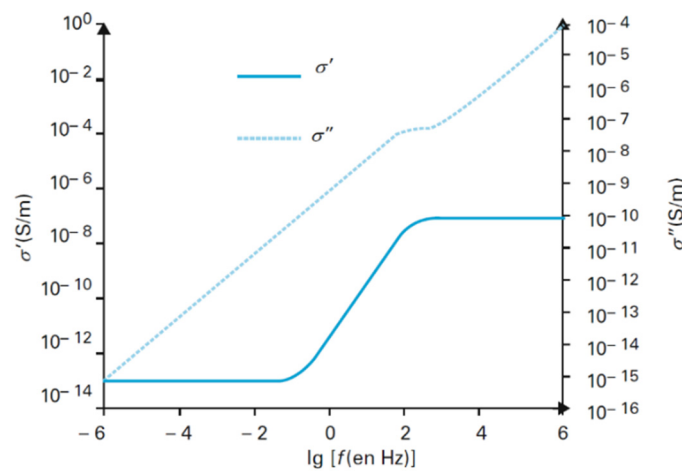


Fig. 4. Frequency spectral signature of real ( $\sigma'$ ) and imaginary ( $\sigma''$ ) conductivities corresponding to a unique relaxation mechanism (Debye) combined to a conduction mechanism [19].

If  $T_u$  is the duration of a voltage cycle, as long as  $t_t \geq \frac{T_u}{2} = \frac{\pi}{\omega}$ , an ohmic regime stands. This regime is therefore present as long as:

$$\sqrt{\frac{\sqrt{2}d^2}{\mu_{ion} 2 \pi f U_{RMS}}} \geq \frac{\pi}{2 \pi f} \tag{14}$$

The value  $f_{threshold}$  of  $f$  for which the two members of the above inequality are equal, and below which the electrode polarization sets up, is:

$$f_{threshold} = \frac{\mu_{ion} U_{RMS} \pi}{2\sqrt{2} d^2} \tag{15}$$

Consequently:

$$\mu_{ion} = \frac{2\sqrt{2} d^2 f_{threshold}}{U_{RMS} \pi} \tag{16}$$

Thus, the value of the frequency corresponding to the onset of electrode polarization, identified from the dielectric spectra and inserted into the above equation (which is derived from the ionic transit time in an ac field), allows assessing the average ionic mobility.

The average diffusion coefficient of the ionic species in the liquid  $D_0$  is then given by the Nernst-Einstein formula:

$$D_0 = k T \mu_{ion} / e_0 \quad (17)$$

where  $k$  is the Boltzmann constant ( $1.38 \times 10^{-23} \text{ J K}^{-1}$ ),  $T$  the absolute temperature of the liquid (in Kelvin) and  $e_0$  the elementary charge ( $1.6 \times 10^{-19} \text{ C}$ ).

Based on the above considerations, the following procedure was employed for acquiring and processing experimental data:

- 1) Measurement of the complex impedance of the empty cell  $Z_0^*$  and determination of the capacitance of the empty cell  $C_0$  in the concerned frequency and temperature ranges.
- 2) Measurement of the complex impedance  $Z^*(f)$  of the cell filled with the liquid sample in the desired frequency and temperature range and determination from  $Z^*(f)$  of the real and imaginary parts of the capacitance  $C'(f)$  and  $C''(f)$ , then determination of the real and imaginary relative permittivity of the material  $\varepsilon_r'(f)$  and  $\varepsilon_r''(f)$  with formula (9)
- 3) Determination of the loss factor  $\tan\delta(f)$  with equation (10).
- 4) Determination of the real and imaginary parts of the conductivity  $\sigma'(f)$  and  $\sigma''(f)$  with equations (12).
- 5) Determination of the static conductivity  $\sigma_{DC}$  as the value of  $\sigma'$  corresponding to the plateau occurring in the low frequency region of the real conductivity spectrum  $\sigma'(f)$ .
- 6) Determination of the frequency  $f_{threshold}$  corresponding to the onset of electrode polarization from the low frequency permittivity spectra of  $\varepsilon_r'$  and  $\varepsilon_r''$ , by considering that the effects of electrode polarization occur as soon as  $\varepsilon_r'$  has increased by 1% compared to its plateau value.
- 7) Determination of the average ionic mobility and diffusion coefficient with equations (16) and (17).

Each one of the spectra presented herein after is the average of three measurements.

### 3. Results and discussion

#### 3.1 Cyclohexane

##### 3.1.1 Liquid cyclohexane

The permittivity and loss spectra of cyclohexane are plotted in Fig. 5 and Fig. 6. For medium and high frequencies (i.e., above 1 Hz), the real permittivity of cyclohexane is practically constant ( $\varepsilon_r \approx 1.9$ ). According to the literature [20–23], temperature variations of  $\varepsilon_r'$  in this frequency range seem to be related to the decrease of the liquid density and to the intervention of complex mechanisms likely to decrease polarizability with temperature. In the low frequency range ( $f < 1 \text{ Hz}$ ), the real permittivity increases when the frequency decreases, reaching values greater than 3 above  $40^\circ\text{C}$ . The imaginary permittivity shows a monotonous decrease as the frequency increases up to 1 kHz. Between 1 kHz and 50 kHz,  $\varepsilon_r''$  is so low that the limits of the measuring device are reached, and the values cannot be exploited. The measuring limits of the apparatus are indicated in grey on the spectra.

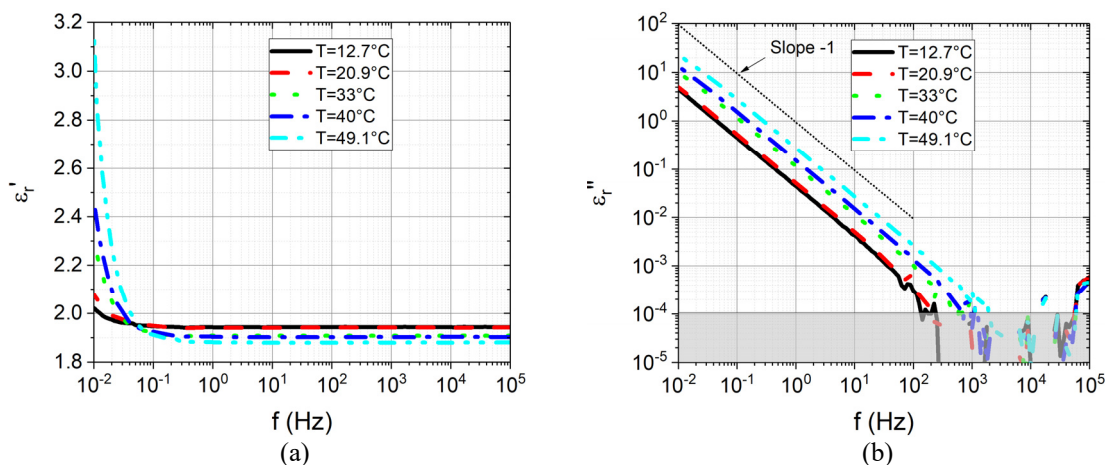


Fig. 5. Spectra of real (a) and imaginary (b) relative permittivity of cyclohexane measured between  $12.7^\circ\text{C}$  and  $49.1^\circ\text{C}$ .

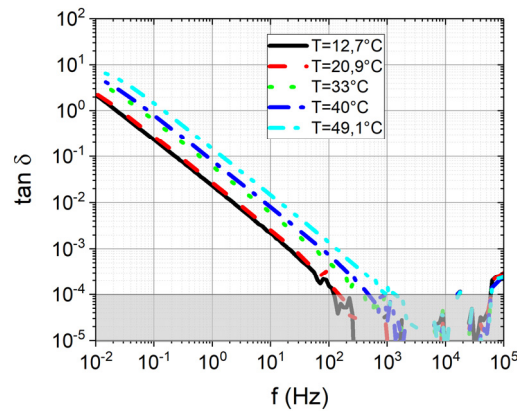


Fig. 6. Loss factor spectra of cyclohexane measured between 12.7°C and 49.1°C.

For all the temperatures, the log-log plots of the variation of  $\epsilon_r''$  with frequency give, below 1 kHz, straight lines of slope equal to  $-1$ , characteristic of a conduction mechanism. Corroborated to a constant value of  $\epsilon_r'$  down to frequency values of 0.02 Hz to 0.5 Hz, this variation highlights a major conduction mechanism in a frequency range between 0.5 Hz and 1 kHz, whatever the temperature.

Below 0.5 Hz, the real permittivity increases significantly with temperature, with a slope of  $\epsilon_r'(f)$  close to  $-1$ . This is a classical behavior of electrode polarization: as the frequency decreases, the duration during which the charge carriers move in the same sense increases, so they get closer and closer to the electrodes of opposite sign during a half cycle. As exposed previously in section 2.3, when frequency falls below a certain threshold, the carriers have time to reach the electrodes of opposite signs during the corresponding half-cycle. For frequencies below this threshold, they accumulate at electrodes, thus increasing the apparent permittivity. This phenomenon is favored by temperature, because the mobility of the ions of the liquid (which are here the main charge carriers) is all the more important as the temperature increases; therefore, they are able to migrate more easily toward the liquid/electrode interfaces and accumulate there.

Table 4. Electrical properties of cyclohexane at different temperatures determined using information obtained by low frequency dielectric spectroscopy.

Temperature (°C)	$f_{threshold}$ (mHz)	$\mu_{ion}$ ( $m^2 V^{-1} s^{-1}$ )	$D_0$ ( $m^2 s^{-1}$ )	$\sigma_{DC}$ ( $S m^{-1}$ )
12.7	30	$3.7 \times 10^{-8}$	$9.1 \times 10^{-10}$	$2.5 \times 10^{-12}$
20.9	50	$6.2 \times 10^{-8}$	$1.6 \times 10^{-9}$	$2.9 \times 10^{-12}$
33.0	70	$8.6 \times 10^{-8}$	$2.3 \times 10^{-9}$	$6.5 \times 10^{-12}$
40.0	120	$1.5 \times 10^{-7}$	$4.0 \times 10^{-9}$	$8.6 \times 10^{-12}$
49.1	160	$2.0 \times 10^{-7}$	$5.5 \times 10^{-9}$	$1.5 \times 10^{-11}$

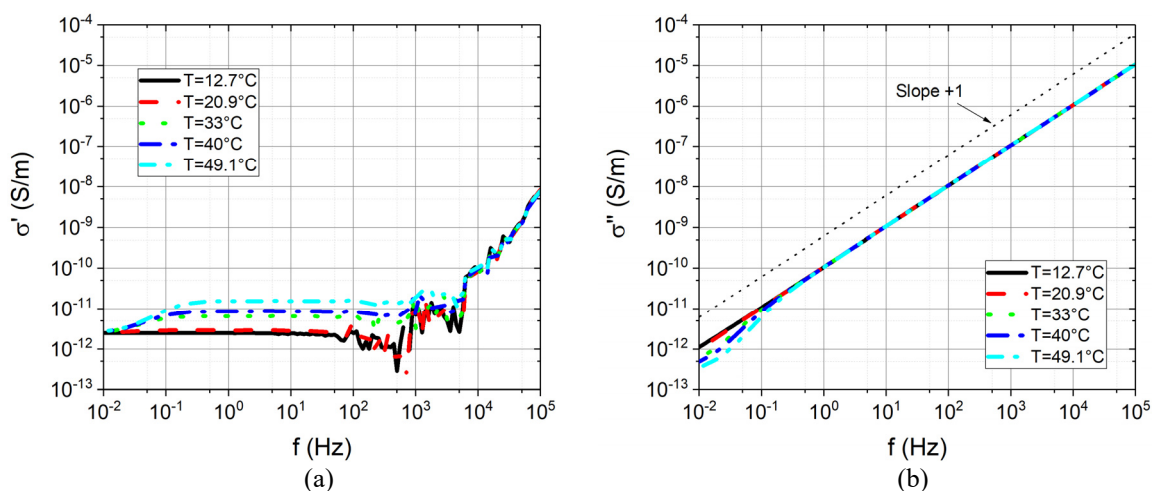


Fig. 7. Spectra of real (a) and imaginary (b) conductivity of cyclohexane measured between 12.7°C and 49.1°C.

By using the electrode polarization onset frequency  $f_{\text{threshold}}$  identified from the permittivity spectra, the average ionic mobility and diffusion coefficients can be determined as proposed in section 2.3. The values thus obtained at the different temperatures are given in Table 4. It can be noted that the values of ionic mobility determined here for cyclohexane are in the range of those obtained for hydrocarbons through other experimental methods (e.g. [1]). They increase with temperature as expected, if only for the decrease of the dynamic viscosity. The diffusion coefficient also increases with temperature, as it is proportional to temperature and mobility.

Fig. 7 presents the real ( $\sigma'$ ) and imaginary ( $\sigma''$ ) conductivity spectra determined from the ( $\sigma'$ ) and ( $\sigma''$ ) spectra with equations (12). For temperatures below 21°C, a wide plateau ranging from  $10^{-2}$  Hz to 1 kHz is observed in the  $\sigma'$  plots. For higher temperatures, this plateau shifts to higher frequencies ( $10^{-1}$  Hz to 70 kHz). As explained before, such plateaus, where the real conductivity does not change with frequency, define the "static" conductivity  $\sigma_{DC}$  [7, 19]. The values of  $\sigma_{DC}$  from Table 4 and plotted in Fig. 8 were obtained.

For frequencies higher than those corresponding to the plateaus, the conductivity  $\sigma'$  increases following a line of slope +1 in log-log coordinates, which corresponds to a law of the type [7]:

$$\sigma' = \sigma_{DC} + A(T) \cdot (2 \pi f)^n \tag{18}$$

with  $n=1$  in this case; the second term thus corresponds to the ac conductivity  $\sigma_{AC} = A(T) \cdot (2 \pi f)^n$  according to the Kremer and Schönhal's definition [7]. The imaginary conductivity  $\sigma''$  is, for its part, increasing with a slope of +1 in the frequency domain corresponding to the plateau of  $\sigma'$  and beyond, as could be expected, given the absence of dielectric relaxations in this domain ( $\epsilon_r' = \text{constant}$ ). The decreases of  $\sigma'$  observed below 0.1 Hz are due to electrode polarization, which artificially decreases conductivity due to the decrease in the number of charge carriers in the liquid moving between electrodes, provoked by the blocking of a fraction of these carriers at electrodes. A variation of the slope of the imaginary conductivity appears in the same region, as expected because of the polarization mechanism [19].

It can be interesting to analyze the origin of the conductivity increase with temperature by using the temperature variation and activation energies of the different parameters involved in the conduction process. Thus, the static conductivity  $\sigma_{DC}$  can be written as:

$$\sigma_{DC} = \sum_i z_i e_0 \mu_{ion_i} n_i \tag{19}$$

where  $z_i$  is the valence of the charge carrier species  $i$  and  $n_i$  its concentration. As mobility  $\mu_{ion}$  is inversely proportional to dynamic viscosity  $\mu_{dyn}$  (the so-called Walden's law), if the conductivity variation is mainly due to the variation of viscosity, the variation of  $\sigma_{DC}(T)$  should be comparable to that of  $1/\mu_{dyn}(T)$ .

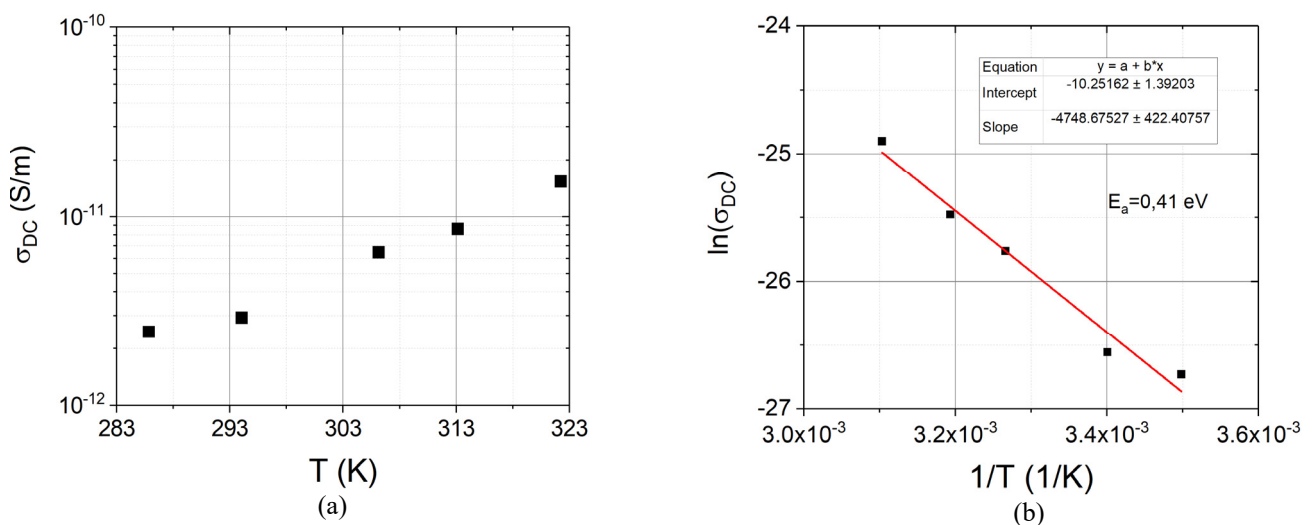


Fig. 8. Variation of the static conductivity  $\sigma_{DC}$  of cyclohexane in the studied temperature range, plotted in Cartesian (a) and Arrhenius (b) coordinates.

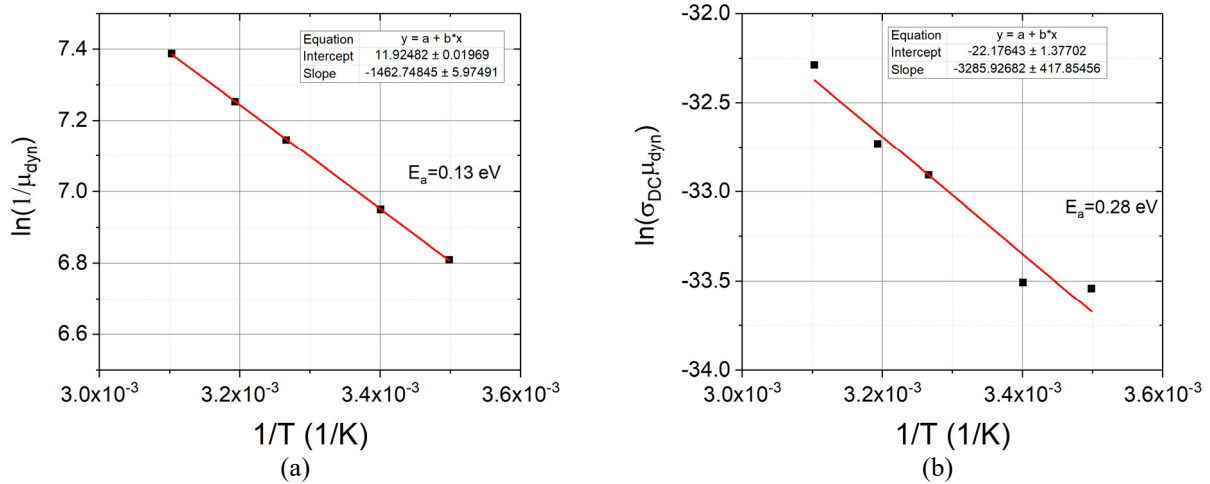


Fig. 9. Temperature variation of the reciprocal of dynamic viscosity (a) and of the product of conductivity by viscosity (b) of cyclohexane, plotted in Arrhenius coordinates.

The Arrhenius plot  $\ln(\sigma_{DC}) = f(1/T)$  from Fig. 8 (b) shows a straight line of slope  $-E_a/k = -4748$ , giving an activation energy  $E_a = 0.41$  eV, corresponding to the orders of magnitude expected for a conduction phenomenon in a liquid. Fig. 9 (a) shows, for the variation of the reciprocal of viscosity  $1/\mu_{dyn}(T)$ , an activation energy  $E_a = 0.13$  eV, much smaller than the one of conductivity, indicating that the conductivity increase with temperature cannot be due only to a decrease of viscosity. On the other hand, the dependence of conductivity on carrier density can be estimated as proposed in [20]: since conductivity  $\sigma_{DC}$  is proportional to the product of the mobility of ions  $\mu_{ion}$  and to the ion density  $n_i$ , and since mobility  $\mu_{ion}$  is inversely proportional to viscosity  $\mu_{dyn}$ , the carrier density should be proportional to the product  $\sigma_{DC}\mu_{dyn}$ . By representing the product  $\sigma_{DC}\mu_{dyn}$  with respect to  $1/T$  (Fig. 9 (b)), one can get an idea on the increase in carrier density under the effect of temperature. Given the level of the activation energies, it seems thus here that the increase in conductivity of cyclohexane with temperature is also significantly promoted by mechanisms leading to carrier generation when temperature raises, rather than being the sole effect of a decrease in viscosity.

### 3.1.2 Solidified cyclohexane

Cyclohexane has a high solidification temperature, near  $6.5^\circ\text{C}$ , which makes it quite easy to set it in solid state to compare to the liquid state. The spectra represented in Figs. 10 – 12 were obtained on cyclohexane solidified in the measurement cell. For this purpose, the thermostatically controlled bath was first cooled down to  $-10^\circ\text{C}$ , then the cell was inserted into the bath and the cell temperature was monitored until the material has reached the desired temperature  $T$ . After a rest time of 30 minutes at  $T$ , the first spectra were measured. The same protocol was used for the other temperatures, without removing the cell from the thermostatically controlled bath.

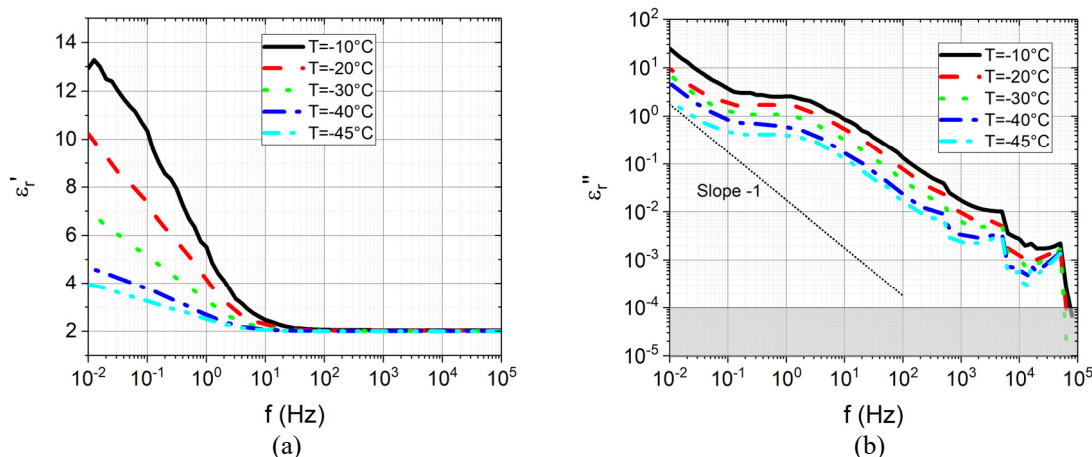


Fig. 10. Temperature variation of the reciprocal of dynamic viscosity (a) and of the product of conductivity by viscosity (b) of cyclohexane, plotted in Arrhenius coordinates.

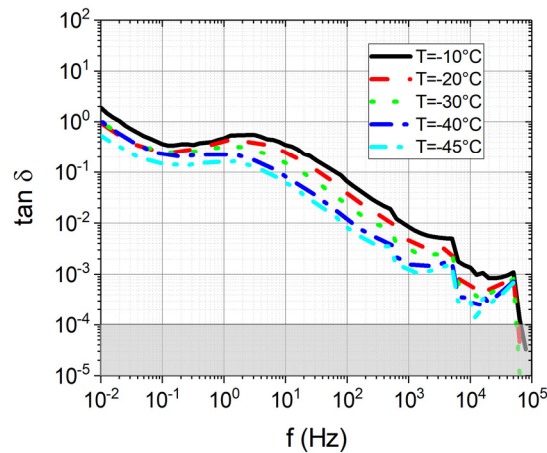


Fig. 11. Loss factor spectra of solidified cyclohexane measured between  $-45^{\circ}\text{C}$  and  $-10^{\circ}\text{C}$ .

The results are very different from those obtained in liquid state. The spectra show a relaxation near 1 Hz, followed by polarization by space and/or electrode charges. In the low frequency range, the values of the real permittivity are much higher than those observed in liquid state (4 to 13 vs. 2 to 3), and decrease with temperature, indicating a shift of the space charge relaxation peak towards lower frequencies, as expected. This behavior is to be related to structural changes in the material due to solidification and to the distribution of ion carriers at the time of solidification.

It is also to be noted that the minimum value of the measurement frequency is not low enough to put into focus a static conductivity plateau (Fig. 12). The static conductivity of solid cyclohexane should therefore be lower than  $10^{-11} \text{ S m}^{-1}$  (and rather close to that of a highly insulating solid polymer, because ionic mobility is very low in solid state and at low temperature, conduction being usually made through electronic mechanisms, where mobility is also very low), which is not surprising considered the values measured in liquid state (e.g.,  $2.46 \times 10^{-12} \text{ S m}^{-1}$  at  $12.7^{\circ}\text{C}$ , see Table 4). To obtain this property (and the others) at low temperatures from the spectra, the frequency range should be extended below  $10^{-2} \text{ Hz}$ , which is feasible with the used apparatus (or with a similar one). Taking into account the high values of  $\epsilon_r$  and  $\epsilon_r''$  measured at  $10^{-2} \text{ Hz}$  and the tendency shown by  $\epsilon_r''$  to increase when frequency decreases, such measurement would likely give exploitable results.

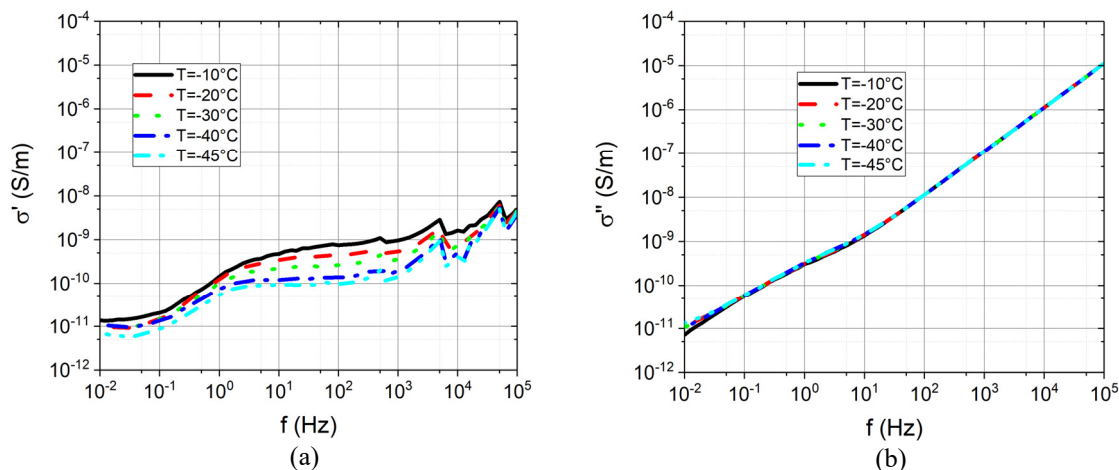


Fig. 12. Spectra of real (a) and imaginary (b) conductivity of solidified cyclohexane measured between  $-45^{\circ}\text{C}$  and  $-10^{\circ}\text{C}$ .

## 3.2 Mineral oil

### 3.2.1 Pure (additive-free) mineral oil

The permittivity and conductivity spectra of the mineral oil are shown in Figs. 13 – 15. The real permittivity is practically constant from 20 mHz to 100 kHz ( $\epsilon_r = 2.16$ ). A major “pure” conduction regime is put into focus

by the permittivity spectra between  $10^{-1}$  Hz and several Hz below  $20^{\circ}\text{C}$ , extended toward 10 Hz and above for temperatures greater than  $20^{\circ}\text{C}$ . This regime also prevails for higher frequencies (up to 100 Hz) at the highest temperatures, but an analysis of the mid frequency range is difficult here due to the small values of the loss factor, which are too low to be accurately determined by the apparatus. A plateau is well identified in the conductivity spectrum in the  $10^{-1}$  Hz...10 Hz range, allowing to determine  $\sigma_{DC}$  at all the temperatures (Table 5). These conductivity values are globally one order of magnitude lower than their cyclohexane counterparts from Table 4, putting into evidence the better insulating properties of the mineral oil. Slight drops of  $\sigma'$  appear below  $10^{-1}$  Hz (especially above  $30^{\circ}\text{C}$ ) due to electrode polarization.

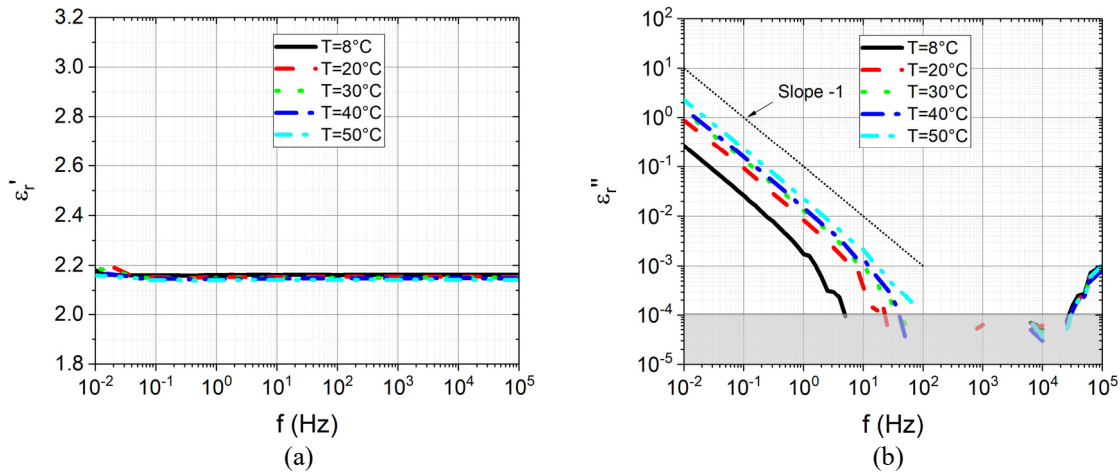


Fig. 13. Spectra of real (a) and imaginary (b) relative permittivity of pure mineral oil measured between  $8^{\circ}\text{C}$  and  $50^{\circ}\text{C}$ .

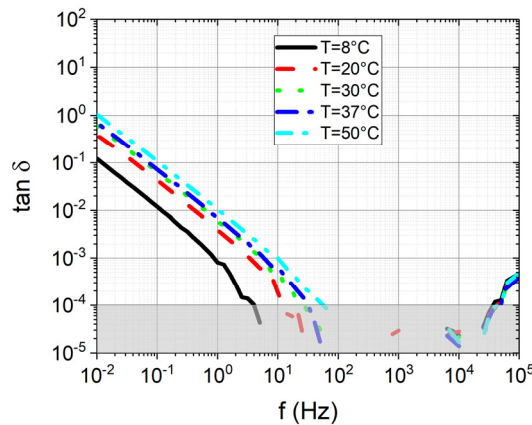


Fig. 14. Loss factor spectra of pure mineral oil measured between  $8^{\circ}\text{C}$  and  $50^{\circ}\text{C}$ .

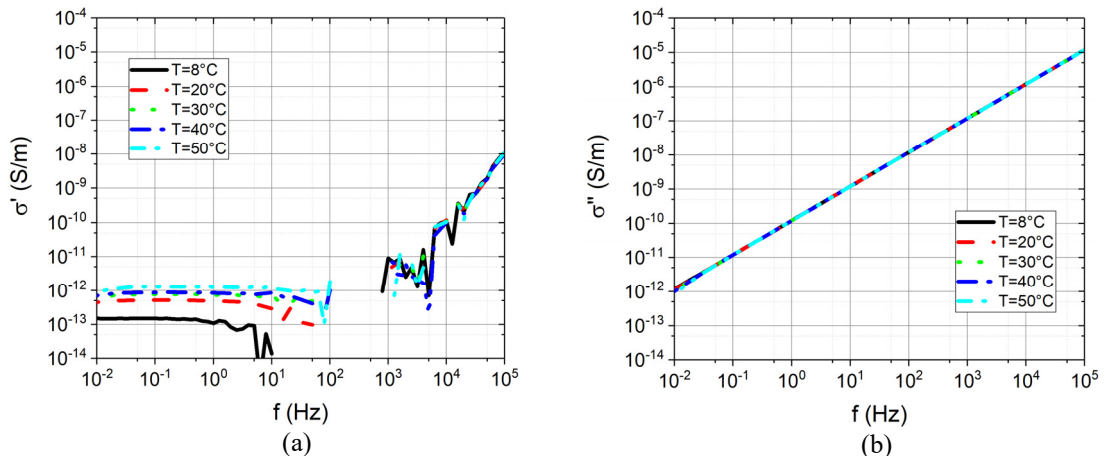


Fig. 15. Conductivity spectra of pure mineral oil measured between  $8^{\circ}\text{C}$  and  $50^{\circ}\text{C}$ .

The values of  $\sigma_{DC}$  are plotted in Fig.16 to underline the influence of temperature. Above room temperature, the variation of  $\sigma_{DC}$  fits an exponential with an activation energy of 0.24 eV, typical of oils [1, 14]. The variation of the dynamic viscosity of this oil [25] shows a slope of 0.28 eV (Fig. 17), suggesting that the variation of the viscosity is a preponderant cause for the conductivity variation above room temperature. A straight drop in conductivity is observed at 8°C, indicating that physical mechanisms related to a decrease in carrier density should also play a significant part at lower temperatures.

A thorough examination of the permittivity spectra seems to show that electrode polarization starts to establish at frequencies in the 20 mHz area. For a polarization onset frequency of 20 mHz, an average mobility of  $2.5 \times 10^{-8} \text{ m}^2 \text{ V}^{-1} \text{ s}^{-1}$  is obtained, which corresponds, at 20°C, to a diffusion coefficient of  $6.2 \times 10^{-10} \text{ m}^2 \text{ s}^{-1}$ . These values are lower than in cyclohexane. They are in the range of data reported in the literature on transformer oils, which indicate diffusion coefficients of the order of  $10^{-9} \text{ m}^2 \text{ s}^{-1}$  to  $10^{-11} \text{ m}^2 \text{ s}^{-1}$  at room temperature (e.g.,  $2.5 \times 10^{-11} \text{ m}^2 \text{ s}^{-1}$  [26]), corresponding to transit times of the order of several hundreds of seconds and more.

However, the small variations of permittivity and conductivity in the lower measurement frequency range makes it difficult to distinguish exact the values of the polarization onset frequency at each temperature, and consequently to determine accurate values for the mobility and the diffusion coefficient at all the temperatures. Indeed, the inflexions in the spectra allowing to identify the setup frequencies for electrode polarization at most of the temperatures are feeble and difficult to put into evidence with the measured data sets (even in  $\partial\epsilon/\partial f = f(f)$  or  $\partial\sigma/\partial f = f(f)$  representations). The measured spectra seem however to indicate that these parameters are close in the studied temperature range, but the resolution in frequency (10 points/decade) and the low frequency limit set for the performed measurements ( $10^{-2}$  Hz) are obviously insufficient to derive them accurately in the case of the mineral oil. This underlines the limits of the proposed method for determining average mobility and diffusion coefficients, which seems to require higher frequency resolutions than 10 points/decade and lower frequency limits (toward  $10^{-3}$  Hz and maybe beyond) in highly insulating liquids. Such measurements would significantly increase the overall time needed for the experiments, but, as already discussed, they should be feasible with instruments as the one used in this work.

Table 5. Static conductivity of mineral oil between 8°C and 50°C determined by low frequency dielectric spectroscopy.

Temperature (°C)	$\sigma_{DC}$ (S m <sup>-1</sup> )
8	$1.5 \times 10^{-13}$
20	$5.2 \times 10^{-13}$
30	$7.7 \times 10^{-13}$
40	$8.8 \times 10^{-13}$
50	$1.3 \times 10^{-12}$

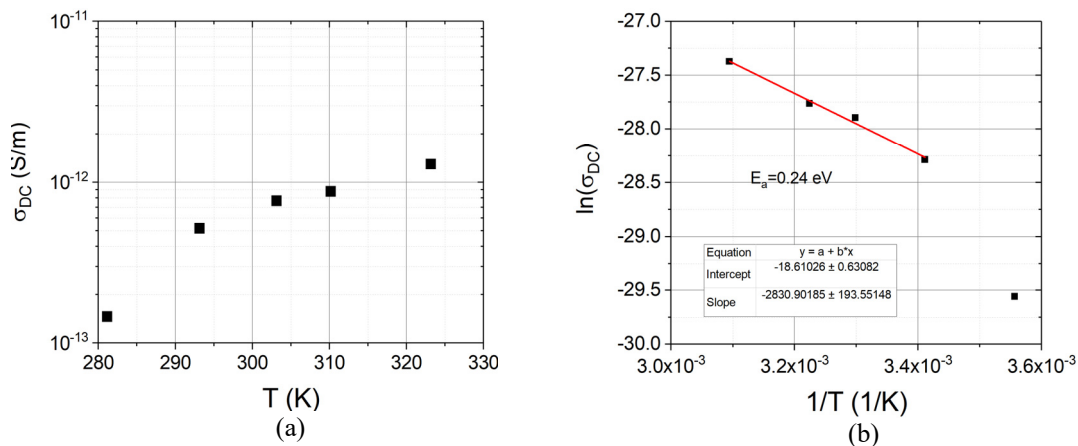


Fig. 16. Variation of the static conductivity of pure mineral oil in the studied temperature range, plotted in Cartesian (a) and Arrhenius (b) coordinates.

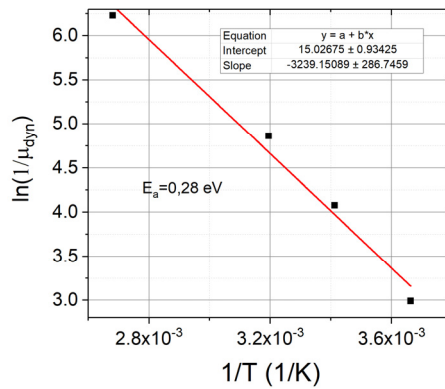


Fig. 17. Temperature variation of the reciprocal of dynamic viscosity of pure mineral oil.

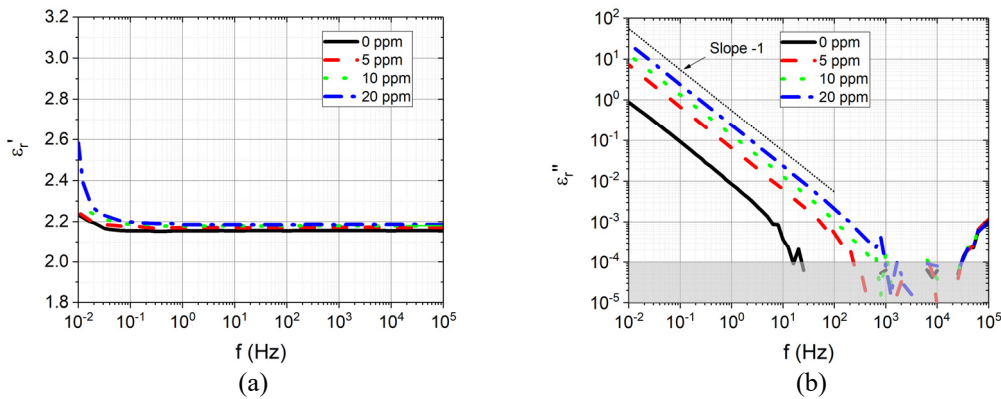


Fig. 18. Spectra of the real (a) and imaginary (b) relative permittivity of mineral oil with and without different amounts of additive, obtained at 20°C.

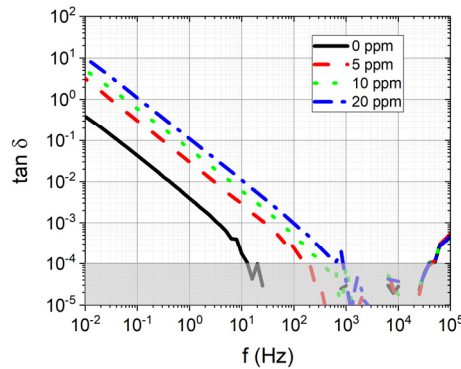


Fig. 19. Loss factor spectra of mineral oil with and without different amounts of additive, obtained at 20°C.

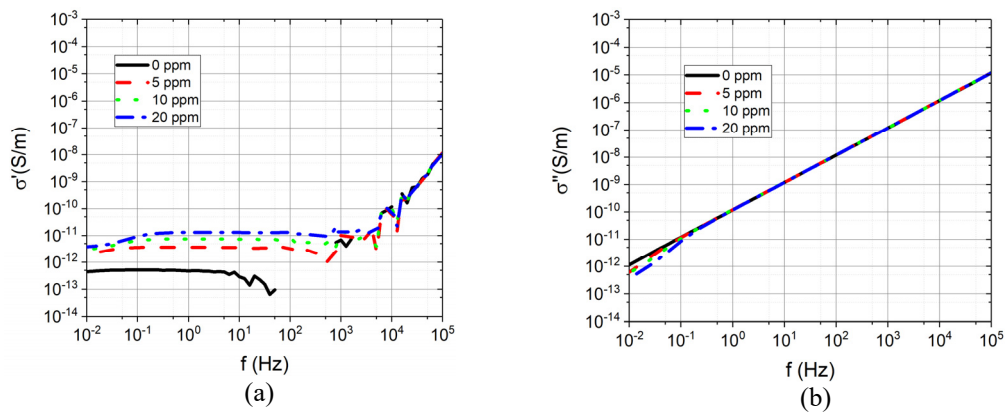


Fig. 20. Spectra of real (a) and imaginary (b) conductivity of mineral oil with and without different amount of additive, obtained at 20°C.

### 3.2.2 Mineral oil with different concentrations of additive

Figs. 18-21 and Table 6 illustrate the spectra and the electrical properties determined for oil samples to which 5 to 20 ppm of additive have been added. The obtained results illustrate the increase of electrode polarization and its onset at higher frequencies, due to the presence of more charge carriers in the liquid under the effect of the additive. Therefore, the static conductivity also increases by almost an order of magnitude when the OLOA 218 is added. It is to note that conductivity increases roughly when 5 ppm of OLOA 218 are added to the pure oil, then by a factor of two each time the concentration of additive doubles, so above there is a quasi-proportionality between conductivity and additive concentration. This indicates that the number of charge carriers appearing in the oil under the effect of the additive is proportional to the concentration of additive. The apparent ion mobility and diffusion coefficients are also higher with respect to the pure oil, but in a much smaller ratio, confirming, if needed, that the conductivity increase is mainly related to the increase in the carrier density under the effect of the additive. The conductivities of the oils with different additive concentrations exhibit similar temperature behaviors and activation energies (0.45 eV, 0.43 eV and 0.56 eV, respectively), which are also close to those of cyclohexane and much higher than the activation energy of the oil viscosity (0.28 eV). This suggests that a carrier density-related behavior like the one in cyclohexane is responsible for the conductivity variation with temperature in the oil to which OLOA 218 has been added

Table 6. Electrical properties at 20°C for the mineral oil with different concentrations of additive determined by low frequency dielectric spectroscopy.

Temperature (°C)	$\sigma_{DC}$ (S m <sup>-1</sup> )	$\epsilon_r$	$f_{threshold}$ (mHz)	$\mu_{ion}$ (m <sup>2</sup> V <sup>-1</sup> s <sup>-1</sup> )	$D_0$ (m <sup>2</sup> s <sup>-1</sup> )
0	$5.2 \times 10^{-13}$	2.16	20	$2.5 \times 10^{-8}$	$6.2 \times 10^{-10}$
5	$3.6 \times 10^{-12}$	2.17	30	$3.7 \times 10^{-8}$	$9.4 \times 10^{-10}$
10	$7.4 \times 10^{-12}$	2.18	46	$5.7 \times 10^{-8}$	$1.4 \times 10^{-9}$
20	$13.2 \times 10^{-12}$	2.19	70	$8.6 \times 10^{-7}$	$2.2 \times 10^{-9}$

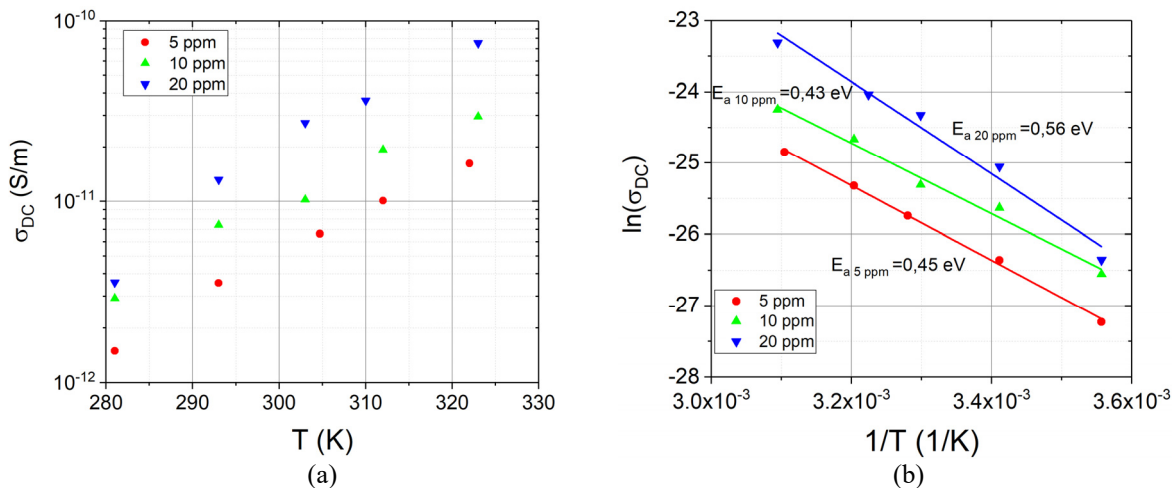


Fig. 21. Variation with temperature of the static conductivity of the mineral oil with different concentrations of additive in Cartesian (a) and Arrhenius (b) coordinates.

### 3.3 Silicon oil

The silicone oil spectra and derived parameters are presented in Fig. 22 to Fig. 24. Below 100 Hz, the imaginary permittivity shows a variation with the logarithm of the frequency with a slope of -1 and the real permittivity is constant down to 20 mHz for all temperatures, putting into evidence a major conduction regime. This allows determining the static conductivities from Table 7, which are in the same range but slightly higher than in mineral oil below 30°C. Above 30°C, they increase faster than in mineral oil, reaching numbers two to three times higher than those of mineral oil. For frequencies higher than 100 Hz, the imaginary values are below the accuracy limits of the apparatus.

As for the pure mineral oil, electrode polarization starts to establish between 20 and 30 mHz at temperatures ranging from 20°C to 50°C. This gives average mobility values of  $2.5$  to  $3.8 \times 10^{-8} \text{ m}^2 \text{ V}^{-1} \text{ s}^{-1}$  (Table 7), similar to the ones for the pure mineral oil, without allowing to accurately separate the values for each temperature because of the low variations and insufficient frequency sampling of the acquired data, as for the mineral oil. For the temperature of 8°C, there is no sign of electrode polarization onset in the spectra, meaning that electrode polarization establishes at frequencies lower than 10 mHz, which gives a mobility value for such low temperatures below  $1.8 \times 10^{-8} \text{ m}^2 \text{ V}^{-1} \text{ s}^{-1}$ .

The activation energy of the conductivity in silicon oil (0.39 eV) is of the same order as those of cyclohexane and additive mineral oil and much higher than that of  $1/\mu_{dyn}$  (around 0.14 eV for this oil if the data from [15] are considered). This leads to the same conclusions as for cyclohexane concerning an important contribution of the increase in the ionic carrier density with temperature to the observed conductivity variation.

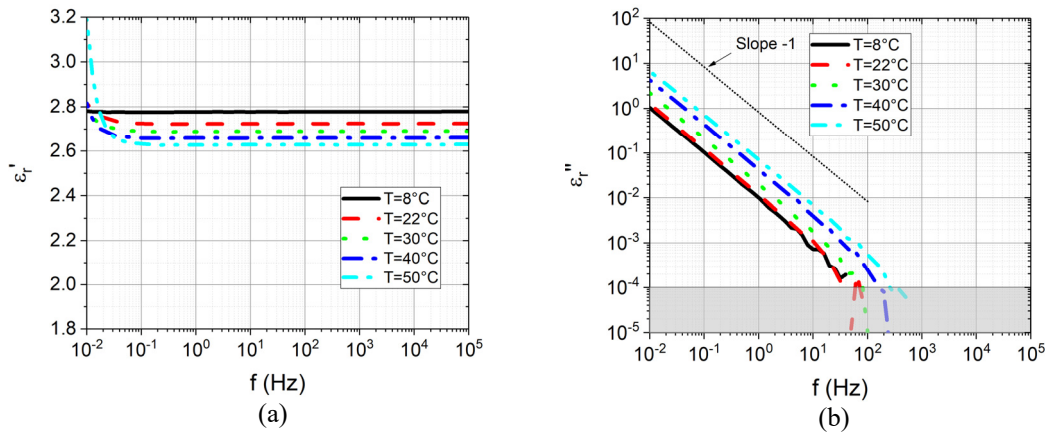


Fig. 22. Spectra of real (a) and imaginary (b) relative permittivity of pure silicone oil measured between 8°C and 50°C.

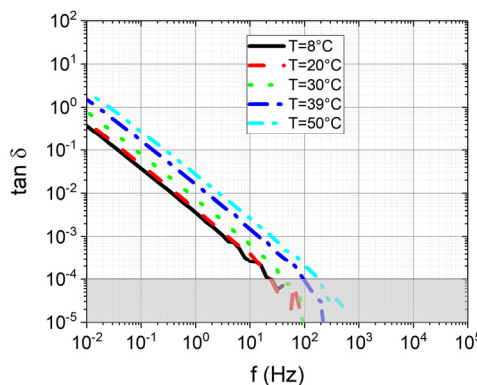


Fig. 23. Loss factor spectra of silicon oil measured between 8°C and 50°C.

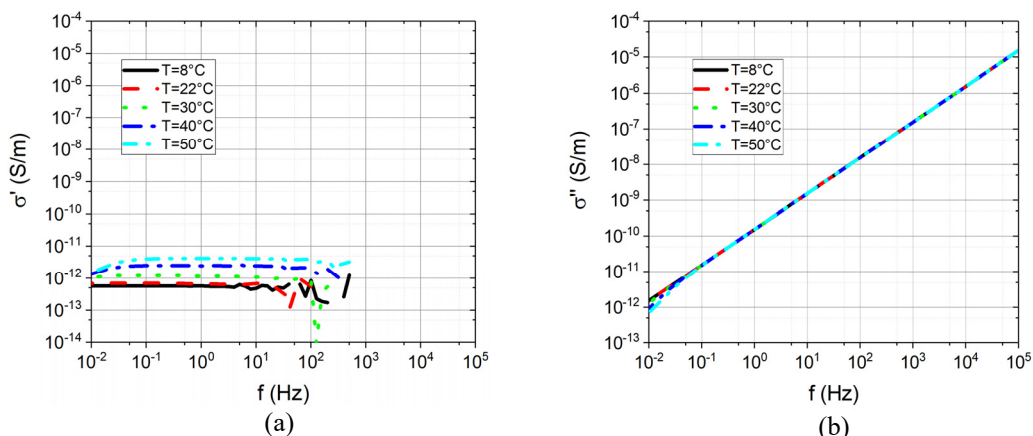


Fig. 24. Conductivity spectra of silicon oil measured between 8°C and 50°C.

Table 7. Electrical properties of silicon oil determined at different temperatures.

Temperature (°C)	$\sigma_{DC}$ (S m <sup>-1</sup> )	$\epsilon_r$	$f_{threshold}$ (mHz)	$\mu_{ion}$ ( $\times 10^{-8}$ m <sup>2</sup> V <sup>-1</sup> s <sup>-1</sup> )	$D_0$ ( $\times 10^{-8}$ m <sup>2</sup> s <sup>-1</sup> )
8	$5.6 \times 10^{-13}$	2.78	< 10	< 1.3	< 3.2
22	$6.5 \times 10^{-13}$	2.73	20	2.5	6.4
30	$1.1 \times 10^{-12}$	2.69	20...30	2.6...3.7	6.5...10
40	$2.4 \times 10^{-12}$	2.66	20...30	2.6...3.7	6.5...10
50	$4.0 \times 10^{-12}$	2.63	30	3.8	11

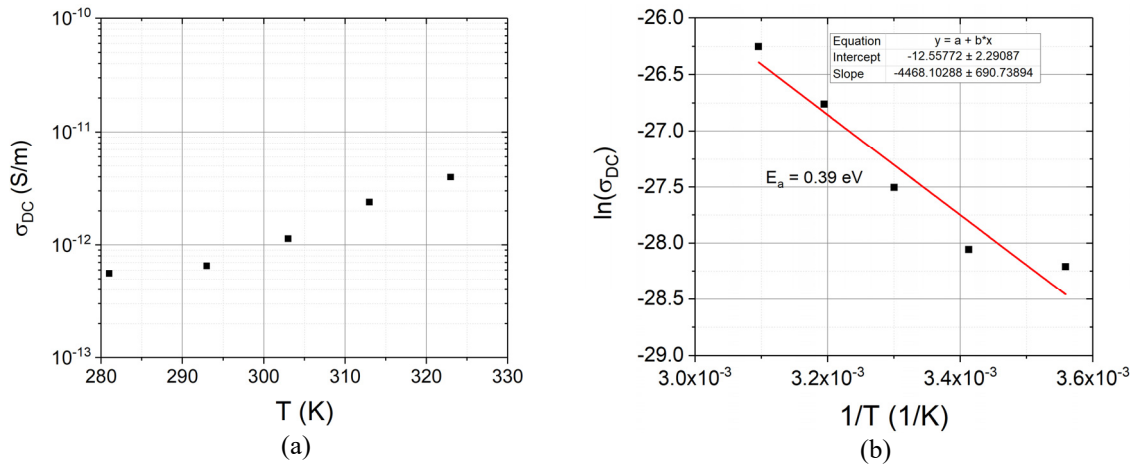


Fig. 25. Variation of the static conductivity of silicone oil with temperature in Cartesian (a) and Arrhenius (b) coordinates.

#### 4. Conclusion

The use of low frequency dielectric spectroscopy for characterizing insulating liquids has been addressed in this paper. The proposed approaches have been first detailed from both theoretical and experimental points of view, then tested on generic insulating liquids as cyclohexane, a mineral oil with and without additives and a silicon oil in a temperature range of 8°C to 50°C. Solidified cyclohexane has also been characterized.

It has been shown that, by using widely available instruments with low frequency capabilities and appropriate analysis of data they can provide, useful electrical properties of such dielectric liquids like electrical conductivity, average mobility and diffusion coefficient can be determined. The obtained results show good agreement with available literature data, and confirm the contributions that such now relatively easy-to-use methods can bring to the study and characterization of dielectric liquids.

#### References

- [1] Bartnikas R., Engineering Dielectrics: Volume III Electrical insulating liquids, 1994.
- [2] Denat A., Etude de la conductivité électrique dans les solvants non polaires, Thèse d'état, Université de Grenoble, 1982.
- [3] Tobazéon R., Etude des phénomènes d'interface au contact d'un liquide isolant et d'un solide, Thèse d'état, Université de Grenoble, 1973.
- [4] Schmidt W., Liquid state electronics of insulating liquids, CRC Press, 1997.
- [5] Hilaire M., Marteau C., and Tobazeon R., Apparatus developed for measurement of the resistivity of highly insulating liquids, *IEEE Trans. Electr. Insul.*, Vol. 23 (4), pp. 779–789, 1988.
- [6] Tobazéon R., Filippini J.C., and Marteau C., On the measurement of the conductivity of highly insulating liquids, *IEEE Trans. Electr. Insul.*, Vol. 1 (6), pp. 1000–1004, 1994.
- [7] Kremer F., and Schönhal A., Broadband dielectric spectroscopy, Springer Berlin Heidelberg, 2003.
- [8] Jonscher A.K., Dielectric Relaxation in Solids, Chelsea Dielectrics Press, 1983.
- [9] Bartnikas R., Dielectric loss in insulating liquids, *IEEE Trans. Electr. Insul.*, Vol. EI-2 (1), pp. 33–54, 1967.

- [10] Neimanis R., Arvidsson L., and Werelius P., Dielectric spectroscopy characteristics of aged transformer oils, Proc. Electrical Insulation Conference and Electrical Manufacturing and Coil Winding Technology Conference, pp. 289–293, 2003.
- [11] Bartnikas R., Some general remarks on the dielectric loss mechanisms in mineral oils, *IEEE Trans. Electr. Insul.*, Vol. 16 (6), pp. 1506–1510, 2009.
- [12] Saturated liquid density - Cyclohexane, (n.d.).  
<http://ddbonline.ddbst.de/DIPPR105DensityCalculation/DIPPR105CalculationCGI.exe?component=Cyclohexane>
- [13] Laurentie J., Chnidir Y., Paillat T., Notingher P., Touchard G., Toureille A., Space charge measurement in liquid dielectrics: numerical and experimental considerations, Proc. ISNPEDAM 2015, La Réunion (France), 2015.
- [14] Leblanc P., Clermont P.D.S., Paillat T., Sidambarompoulé X., Laurentie J., and Notingher P., Numerical study of the thermal excitation applied to a dielectric liquid film, 2019 IEEE 20th International Conference on Dielectric Liquids (ICDL), 2019.
- [15] Rhodorsil® Huiles 47 V 50 à 47 V 1000 - Fiche Technique n° SIL03241 1, 2004.  
[http://www.silitech.ch/upload/complement\\_info\\_fournisseur\\_d/32.pdf](http://www.silitech.ch/upload/complement_info_fournisseur_d/32.pdf)
- [16] Moretto H.-H., Schulze M., Wagner G., Silicones, Ullmann's encyclopedia of industrial chemistry, American Cancer Society, 2000.
- [17] CEI 60247, Liquides isolants – Mesure de la permittivité relative du facteur de dissipation diélectrique (tan delta) et de la résistivité en courant continu, Commission Electrotechnique Internationale, 2004.
- [18] Cellule de laboratoire à très faibles pertes pour la mesure de la conductivité et du facteur de dissipation des liquides très isolants - Type CL-1, Technical Datasheet, 2007.
- [19] Gallot-Lavallee O., and Gonon P., Caractérisation des polymères par spectroscopie diélectrique, Techniques de l'ingénieur - Propriétés Générales Des Plastiques, Base documentaire TIB152DUO, 2016.  
<https://www.techniques-ingenieur.fr/base-documentaire/materiaux-th11/proprietes-generales-des-plastiques-42152210/caracterisation-des-polymeres-par-spectroscopie-dielectrique-am3141/>
- [20] Muslim J., Hanna R., Lesaint O., Reboud J.L., and Sinisuka N.I., Electrical characterization of synthetic ester liquid over wide temperature range (–60°C/200°C), 2017 IEEE 19th International Conference on Dielectric Liquids (ICDL), pp. 1–4, 2017.
- [21] Mopsik F.I., Dielectric constant of N-hexane as a function of temperature, pressure, and density, *J. Res. Natl. Stand., Sec. A*, Vol. 71A (4), pp. 287–292, 1967.
- [22] Scaife W.G., Relative permittivity of organic liquids as a function of pressure and temperature, 1971.
- [23] Garg S.K., Bertie J.E., Kilp H., and Smyth C.P., Dielectric relaxation, far-infrared absorption, and intermolecular forces in nonpolar liquids, *J. Chem. Phys.*, Vol. 49 (6), pp.2551–2562, 1968.
- [24] Clermont P.D.S., Paillat T., and Leblanc P., Numerical study on the impact of a temperature step on the electrical double layer, *J. Electrostat.* Vol. 95, pp.13–23, 2018.
- [25] Shell Diala S2 ZX-A, Technical Data Sheet, Shell, 2018.
- [26] Lyon D.J., Melcher J.R., Zahn M., Couette charger for measurement of equilibrium and energization flow electrification parameters: application to transformer insulation, *IEEE Trans. Electr. Insul.*, Vol. 23 (1), pp.159–176, 1988.